IMEKO International Conference on
Metrology for Archaeology and Cultural Heritage
Lecce, Italy, October 23-25, 2017

New crack measurement methodology: Tag Recognition

Fabio Mangini[1,2,3], Lorenzo Dinia[1], Fabrizio Frezza[1], Andrea Beccarini[3], Mauro Del Muto[3], Enrico Federici[3], Stefano Godi[3], Andrea Segneri[3,4]

[1]*Department of Information Engineering, Electronics and Telecommunications, "La Sapienza" University of Rome, Via Eudossiana 18, 00184 Roma, Italy.*
[2]*Enrico Fermi Center - Museo Storico della Fisica e Centro Studi e Ricerche "Enrico Fermi", Piazza del Viminale 1, 00184 Roma, Italy.*
[3]*Step Over, Via Aulo Plauzio 6, 00181 Roma, Italy.*
[4]*Heriot Watt University, Edinburgh Campus, Edinburgh EH14 4AS, United Kingdom.*

***Abstract* – In this paper, a new methodology for measuring the cracking for the Structural Health Monitoring (SHM) of cultural heritage, is presented. This methodology is characterized by being minimally invasive on the artifact to preserve, which is one of the main qualities required in this field. The approach used is to determine the relative distance between two optical tags, using advanced fitting algorithms for the objective function. In this work, we have taken into account different objective-function kinds, in order to find the best configuration to determine the fitting parameters, useful to the SHM. In order to validate the fitting algorithms, some measurements evaluated on simulated tags are presented. Moreover, to validate the methodology, some real measurements are shown.**

I. INTRODUCTION

The traditional approach used in SHM involves performing static and dynamic tests and measures, occasionally or periodically, but with typically long periods of time. Static monitoring techniques aim at detecting the structural characteristics (slow deformation and displacement) of a structure and subjecting to test loads of intensity such as to induce, by simulating variable operating actions, the maximum stresses projected at the design stage. This technique is then coupled with a measuring instrument composed of strain gauges (linear potentiometric extensimeters, resistive extensometers, capacitive extensometers, linear variable displacement transducer, fiber optic extensometers, FBG) and thermometers to take into account the possible thermal expansion of the materials to which the other sensors are fixed. Dynamic tracking techniques aim at determining the dynamic response of the structure through accelerometers, inclinometers, piezometric extensometers (or, alternatively, speed or displacement gauges, from which) [1, 2, 3, 4, 5]. Despite that with these techniques, it is possible to carry out thorough investigations into the state of an infrastructure, they have a large amount of invasiveness, both in terms of mass, in terms of anchorage on artifact and in visual impact. For this purpose, the so-called Optical Tags are introduced. The tags are nothing but adhesive labels with appropriate images, through which, by using advanced fitting methods and algorithms, it is possible to determine the absolute and relative position and three-dimensional rotations of the image itself.

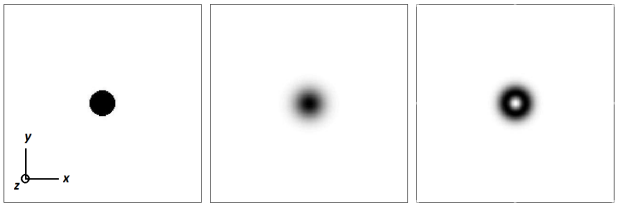

Fig. 1. Optical tag profiles: circular tag, gaussian tag, laplacian tag.

II. TAG SELECTION

A couple of years ago a paper was published where a similar approach was used in astrophysics in order to determine the position of the stars from high definition telescope images [6]. Their method was based on the reconstruction by the fitting of the point spread function (PSF). Their hypothesis is based on the fact that the image of the stars could be considered with a good approximation as a two-dimensional Gaussian distribution. In our case, having no constraints on the shape of the objective function, the first step was to determine the best distribution to be used as a target. Given the circular symmetry of the same, the following functions have been chosen:

$$f(x,y) = A|(x-x_o)^2 + (y-y_0)^2| \leq r^2 \qquad (1)$$

$$f(x,y) = Ae^{-\left[\frac{(x-x_O)^2}{2\sigma_x^2} + \frac{(y-y_O)^2}{2\sigma_y^2}\right]} \qquad (2)$$

$$f(x,y) = A\left[\frac{(x-x_o)^2}{\sigma_x^3} - \frac{(y-y_o)^2}{\sigma_y^3}\right] e^{-\frac{(x-x_o)^2}{2\sigma_x^2} - \frac{(y-y_o)^2}{2\sigma_y^2}} \quad (3)$$

having indicated with $f(x,y)$ the circular function, Gaussian function and a linear combination of the Laplacian of Gaussian and Gaussian ones (which we will simply call Laplacian for simplicity), respectively. The three tag profiles are shown in Fig. 1. For the determination of the best typology of tags, constant-speed translational tests are performed, considering a simulated tag starting from the formulas previously described. To simulate a real tag, we have started from an ideal tag $f(x,y)$ and we have added a vertical translation z_0 and a random noise $r(x,y)$ equal to 10% of the maximum value: $F(x,y) = f(x,y) + z_0 + r(x,y)$.

III. METHODS AND MEASURES

The method used to determine the displacement, i.e. the parameters x_0 and y_0 and the standard deviations (σ_x e σ_y), from which it is possible to determine rotations around the x and y-axes (see Fig. 1) is the method of data fitting of the minimum squares applied to non-linear curves. In particular, two methodologies were adopted in this context; the first one is the nonlinear solving least-squares method based on the algorithm of the "trust-region-reflective" [7] and the second one is based on the algorithm of "Levenberg-Marquardt" [8, 9, 10]. Thanks to these methods it is possible to determine the parameters A, x_0, y_0, σ_x, and σ_y. Comparisons were performed between images with different resolution, in particular: 100×100, 200×200 and 400×400 px of resolution, a vertical translation z_0 equal to the 20% of the maximum value and a random noise $r(x,y)$ equal to 10% of the maximum value. The tag position variation was performed along the bisector with tens of pixel variations. The results obtained are shown in the tables 1, 2 and 3 for 100×100, 200×200 and 400×400 px of resolution, respectively.

How we can see from the results in tables (1, 3 ,and 3), the percentage of the absolute error compared to the displacement of 0.1 px improves proportionally with increasing image resolution. Moreover, there aren't appreciable differences between the two methodologies in order to determine the tag position.

Finally, we simulate in a controlled environment a crack enlargement (see Fig. 2). The system is constituted by a video capture system GigE Vision Mako G (some tests are performed using IPcam of Netsurveillance codec h264), a power supply channel and data exchange via Ethernet cable (PoE, Power over Ethernet), a PC for running the fitting algorithm (but a single-board computer is usable as well), and in order to simulate the controlled displacement of the tags we have positioned an HD video at a distance of 1 m, where were reproduce two Gaussian tags. We have considered only a displacement along the x-direction of two

Table 1. Percentage of the absolute error compared to the displacement of 0.1 px of the fitting parameters in the case of 100×100 *px of resolution, using a) Trust-region-reflective, 2) Levenberg-Marquardt algorithm*

	Trust-region-reflective method		
	Circular	Gaussian	Laplacian
$\lvert x_i - x_o \rvert$	65.02%	42.74%	24.56%
$\lvert y_i - y_o \rvert$	60.45%	48.42%	29.88%
$\lvert \sigma_{x_i} - \sigma_{x_o} \rvert$	×	52.35%	15.71%
$\lvert \sigma_{y_i} - \sigma_{y_o} \rvert$	×	51.97%	16.65%
	Levenberg-Marquardt method		
	Circular	Gaussian	Laplacian
$\lvert x_i - x_o \rvert$	67.40%	45.63%	26.15%
$\lvert y_i - y_o \rvert$	68.45%	44.68%	25.74%
$\lvert \sigma_{x_i} - \sigma_{x_o} \rvert$	×	48.31%	15.06%
$\lvert \sigma_{y_i} - \sigma_{y_o} \rvert$	×	56.70%	14.98%

Table 2. Percentage of the absolute error compared to the displacement of 0.1 px of the fitting parameters in the case of 200×200 *px of resolution, using a) Trust-region-reflective, 2) Levenberg-Marquardt algorithm*

	Trust-region-reflective method		
	Circular	Gaussian	Laplacian
$\lvert x_i - x_o \rvert$	33.27%	19.30%	12.30%
$\lvert y_i - y_o \rvert$	79.95%	21.05%	10.90%
$\lvert \sigma_{x_i} - \sigma_{x_o} \rvert$	×	33.71%	8.74%
$\lvert \sigma_{y_i} - \sigma_{y_o} \rvert$	×	31.87%	9.40%
	Levenberg-Marquardt method		
	Circular	Gaussian	Laplacian
$\lvert x_i - x_o \rvert$	15.63%	20.26%	12.17%
$\lvert y_i - y_o \rvert$	35.88%	22.38%	11.96%
$\lvert \sigma_{x_i} - \sigma_{x_o} \rvert$	×	33.10%	8.44%
$\lvert \sigma_{y_i} - \sigma_{y_o} \rvert$	×	36.94%	8.90%

Gaussian tags. The resolution of the ROI (Region Of Interest) acquired is 400×400 px. It was considered a displacement step by a pixel (with respect to the monitor tags resolution), for a complex 10 pixel shift (see Figs. 3,4). In the figures 3 and 4 we can see the initial and final position of the tags in an ROI of 400×400 px size, the right tag does not undergo movement. The double Gaussian curves represent the acquired image and the reconstructed image with Levenberg-Marquardt fitting algorithm, both passing through the maximum values.

In fig. 5 we can see the relative error between the effective displacement and the displacement computed with respect to the two directions. In particular, the upper plot with respect to the y-direction and the middle plot respect the x-direction. In the lower plot, we can see the graph of measured displacement in the pixel as a function of the effective displacement in a tenth of a pixel. The dependence between the two values is perfectly linear in the range of

Table 3. Percentage of the absolute error compared to the displacement of 0.1 px of the fitting parameters in the case of 400×400 *px of resolution, using a) Trust-region-reflective, 2) Levenberg-Marquardt algorithm.*

	Trust-region-reflective method		
	Circular	Gaussian	Laplacian
$\lvert x_i - x_o \rvert$	16.01%	9.16%	5.21%
$\lvert y_i - y_o \rvert$	36.77%	8.32%	4.23%
$\lvert \sigma_{x_i} - \sigma_{x_o} \rvert$	×	16.18%	4.55%
$\lvert \sigma_{y_i} - \sigma_{y_o} \rvert$	×	16.26%	4.29%
	Levenberg-Marquardt method		
	Circular	Gaussian	Laplacian
$\lvert x_i - x_o \rvert$	15.63%	9.41%	5.76%
$\lvert y_i - y_o \rvert$	35.88%	10.17%	6.00%
$\lvert \sigma_{x_i} - \sigma_{x_o} \rvert$	×	16.71%	4.88%
$\lvert \sigma_{y_i} - \sigma_{y_o} \rvert$	×	17.86%	4.94%

Fig. 2. In vivo test system.

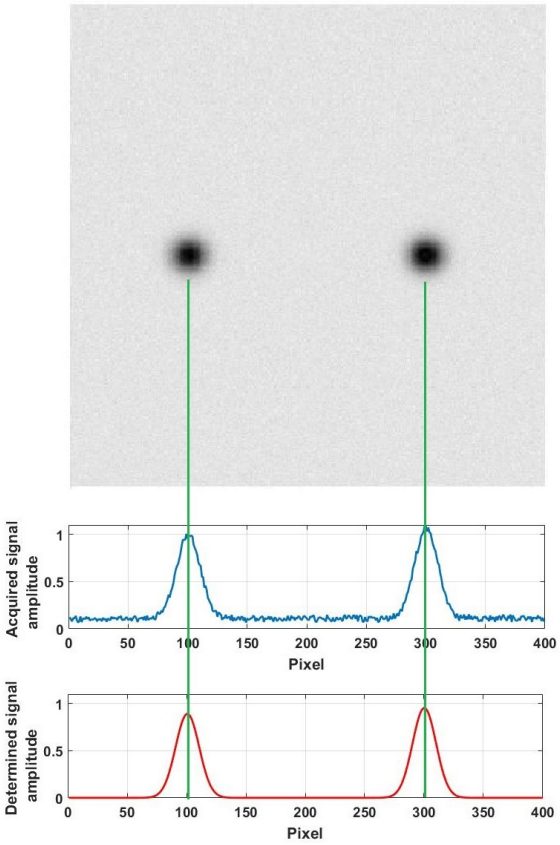

Fig. 3. Initial tags position acquired. The upper graph represents the signal image acquired along the central row. The lower graph represents the reconstructed image after the Levenberg-Marquardt fitting algorithm along the same row.

shift taken into account. Moreover, the mean value of the relative error with respect to the two directions is present.

IV. CONCLUSIONS

In conclusion, we can assert that the best tag is the Laplacian one and that the best algorithm is the "trust-region-reflective", even if the differences are minimal, but with a double processing speed. We also found that when the image resolution increases, the relative error is reduced for both translation and variation of standard deviation. Thus we can say that this relative distance measurement methodology can be satisfactorily used for SHM, in particular, to monitor the cracks of Cultural Heritage, i.e. in order to monitor the micro-displacement, for example, due to bradisismic phenomena. It is effectively integrated among other established structural monitoring methods having different economic and metrological characteristics compared to all other measurement techniques.

REFERENCES

[1] V. Gattulli, M. Lepidi, and F. Potenza, "Dynamic testing and health monitoring of historic and modern civil structures in Italy," Structural Monitoring and Maintenance, 2016.

[2] C. Gentile, M. Guidobaldi, and A. Saisi, "A One-year dynamic monitoring of a historic tower: damage detection under changing environment," Meccanica, 2016.

[3] M.-G. Masciotta, J.C.A. Roque, L.F. Ramos, and P.B. Lourenço, "A multidisciplinary approach to assess the health state of heritage structures: The case study of the Church of Monastery of Jerónimos in Lisbon," Construction and Building Materials, 2016.

[4] J. Garcia-Palacios, J.M. Soria, I.M. Díaz, and F. Tirado-Andrés, "Modal tracking with only a few of sensors: Application to a residential building," 8th European Workshop on Structural Health Monitoring, EWSHM 2016.

[5] A. Saisi, M. Guidobaldi, and C. Gentile, "On site investigation and health monitoring of a historic tower in Mantua, Italy," Applied Sciences, 2016.

[6] R. Suszynsk and K. Wawryn, "Stars' Centroid Deter-

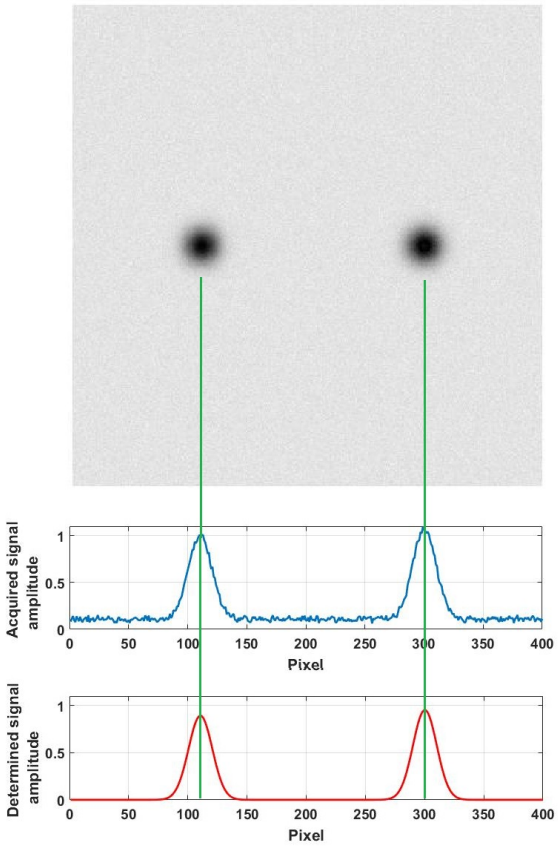

Fig. 4. Final tags position acquired. The upper graph represents the signal image acquired along the central row. The lower graph represents the reconstructed image after the Levenberg-Marquardt fitting algorithm along the same row.

mination Using PSF-Fitting Method," Metrology and Measurement Systems, Vol. 22, No. 4, pp. 547-558, 2015.

[7] J.J. Moré, "The Levenberg-Marquardt Algorithm: Implementation and Theory," Numerical Analysis, ed. G. A. Watson, Lecture Notes in Mathematics 630, Springer Verlag, 1977, pp. 105-116.

[8] J.E. Jr Dennis, . "Nonlinear Least-Squares," State of the Art in Numerical Analysis, ed. D. Jacobs, Academic Press, pp. 269-312.

[9] K. Levenberg, "A Method for the Solution of Certain Problems in Least-Squares," Quarterly Applied Mathematics 2, 1944, pp. 164-68.

[10] D. Marquardt, "An Algorithm for Least-squares Estimation of Nonlinear Parameters," SIAM Journal Applied Mathematics, Vol. 11, pp. 431-441, 1963.

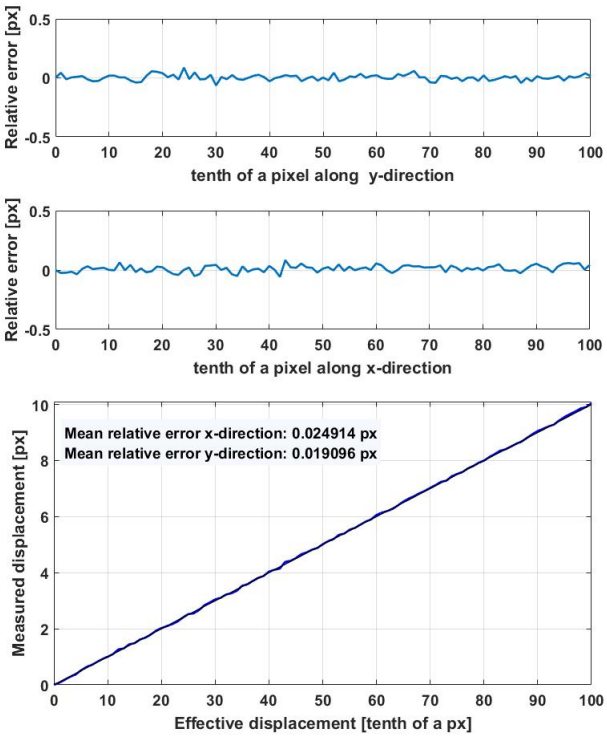

Fig. 5. Relative error between the effective displacement and the displacement computed with respect to the two directions. In the lower plot: the graph of measured displacement in the pixel as a function of the effective displacement in tenth of a pixel.